Talanta 209 (2020) 120611

Contents lists available at ScienceDirect

Talanta

journal homepage: www.elsevier.com/locate/talanta

Peptide-conjugated hemin/G-quadruplex as a versatile probe for "signal-on" electrochemical peptide biosensor

Zhuo Ye[a], Gaiping Li[a], Lingling Xu[a], Qian Yu[a], Xiaoyue Yue[b], Yongmei Wu[b,**], Baoxian Ye[a,*]

[a] The First Affiliated Hospital, Department of Chemistry, Zhengzhou University, Zhengzhou, 450001, China
[b] College of Food and Biological Engineering, Zhengzhou University of Light Industry, Zhengzhou, 450001, China

ARTICLE INFO

Keywords:
Peptide-conjugated DNAzyme
Electrochemistry
Peptide biosensor
High sensitivity
Prostate-specific antigen

ABSTRACT

In this work, a novel "signal-on" electrochemical peptide biosensor based on peptide-conjugated hemin/G-quadruplex (DNAzyme-peptide) hybrid and rosebud-like $MoSe_2$@reduced graphene oxide ($MoSe_2$@rGO) nanocomposite, was developed for detection of prostate-specific antigen (PSA). Interestingly, the peptide not only served as recognition probe to detect PSA, but also acted as the enhancer to improve the enzyme activity of hemin/G4, which promoted the detection sensitivity. Up addition of PSA, Fe_3O_4-labeled DNAzyme-peptide probe was cleaved, followed by the magnetic separation. The cleaved DNAzyme-peptide was then captured onto the cysteine-modified electrode via the interaction between carboxyl groups of peptide and amino group of cysteine. A strong electrochemical signal was obtained from hemin and further was amplified by the enhanced electrocatalysis of DNAzyme-peptide. Compared to the original DNAzyme, DNAzyme-peptide exhibited more than 3-fold enhancement in signal amplification. And $MoSe_2$@rGO amplified the electrochemical signal due to its good conductivity and large surface area. So the proposed strategy detected PSA down to 0.3 fg/mL, and it showed the advantages of simplicity, low cost by avoiding the use of expensive protein enzyme and additional electroactive species. Therefore, the proposed biosensor potentially provided a very effective tool for early diagnosis of cancer by the detection of PSA.

1. Introduction

In clinical, prostate-specific antigen (PSA) has become the best available biomarker to diagnose prostate disease, monitor the disease progression and evaluate therapeutic response [1]. So, developing a simple, fast and effective tool for detection of PSA is highly necessary in diagnostic devices. Various oligopeptides as recognition probe have been progressively integrated into biosensor design to assay protein [2–6] because peptide has defined chemical structure, high affinity and specificity for target molecules and the target range is relatively wide due to the diversity of amino acids. Especially, electrochemical peptide biosensors are fast, more sensitive, convenient, and have increasingly attracted attention in quantifying the levels of proteins [7–10]. Unfortunately, most of these biosensors are mainly based on "signal-off" sensing mechanism, which may result in the limited sensitivity and "false positive" results. Until recently, Yuan's group [11–13] have established "signal-on" mode detecting protein based on magnetic bead-labeled peptide probe, while several limitations still existed in these strategies. For example, the absence of signal amplification rendered this biosensor low-sensitivity [11]. The use of expensive and easily denatured protein enzyme (i.e., ExoIII, nicking enzyme and polymerase), might bring about false signal, increased reagent cost, and cumbersome preparation of additional signal reporter (methylene blue/ferrocene-labeled DNA)[12,13]. Therefore, exploring a more effective signal amplification method is still to be challenged in "signal-on" electrochemical peptide biosensor.

Hemin/G-quadruplex (hemin/G4) DNAzyme has been extensively employed as biocatalyst to enhance the detection sensitivity of biosensor due to its several advantages such as easy synthesis, small size, low cost, good chemical stability and peroxidase-like activity [14–18]. Nevertheless, the lower biocatalytic activity of G4 DNAzyme over its protein counterpart discounts the sensitivity. In response to the above arguments, hemin/G4-peptide with superior performance was synthesized according to a previous work [19] using cationic peptide to enhance enzyme activity, and it was employed to develop electrochemical aptasensor in our previous studies [20,21]. But not all of our previous strategies were cost-effective and simple for biological detection, given that the peptide was only used as enzyme activity enhancer and

* Corresponding author.
** Corresponding author. College of Food and Biological Engineering, Zhengzhou University of Light Industry, Zhengzhou, 450001, China.
E-mail addresses: wuyongmei0001@163.com (Y. Wu), yebx@zzu.edu.cn (B. Ye).

https://doi.org/10.1016/j.talanta.2019.120611
Received 20 September 2019; Received in revised form 28 November 2019; Accepted 1 December 2019
Available online 02 December 2019
0039-9140/

additional aptamer was still needed to detect target. Peptides are modular and each unit can carry out its own intrinsic function independent of adjacent units [22]. Thus, we imagined that if a bifunctional peptide consisting of protein-recognition motif and cationic peptide motif, was conjugated to G4 structure and then bound with hemin, how about the DNAzyme-peptide hybrid? Firstly, the protein-recognition motif could be used for detection of target protein. Secondly, owing to presence of cationic peptide, the bifunctional peptide was expected to enhance the DNAzyme activity, so as to improve the capability of DNAzyme to amplify signal. Furthermore, the intercalated hemin could provide a detectable electrochemical signal because of its redox activity. As such, the DNAzyme-peptide hybrid held promise as high-efficiency bioprobe for developing a simple yet sensitive peptide biosensor. To the best of our knowledge, no attention is paid to the application of such a versatile DNAzyme-peptide in "signal-on" electrochemical peptide biosensor.

To obtain a better performance, additional nanomaterials with unique properties, have been typically employed in biomolecular detection to enhance the electron transfer, increase the immobilization amount of probe and amplify the response signal. For example, MoS_2 nanomaterials have gained increasing attention in sensing applications due to its graphene-like structure, high surface-to-volume ratios and electrocatalytic activity toward H_2O_2 [23–27]. Whereas, the electronic conductivity of MoS_2 is not good, and the poor electrical contact between active sites on the lying architectures may suppress their electrocatalytic activities, which are not conducive to the improvement of sensor performance. Alternatively, $MoSe_2$ has a better conductivity due to the higher metallic property of Se [28], and the combination of three-dimensional (3D) $MoSe_2$ nanomaterials and electrically conductive reduced graphene oxide (rGO), can provide more active reaction sites and accelerate electron transfer [29]. Therefore, 3D $MoSe_2$@rGO nanostructure was considered as an ideal substrate material for constructing electrochemical biosensing platform.

In this work, we elaborately conjugated a bifunctional peptide, which consisted of cationic peptide and PSA-recognition peptide (HSSKLQ) [30], to hemin/G4 DNAzyme and combined the DNAzyme-peptide with rosebud-like $MoSe_2$@rGO to develop a "signal-on" electrochemical peptide biosensor with excellent performance (Scheme 1). The DNAzyme-peptide hybrid was first labeled with Fe_3O_4–COOH sphere, resulting in the formation of magnetic DNAzyme-peptide-Fe_3O_4 probe. In the presence of PSA target, the protein-recognition peptide in magnetic probe was cleaved, which caused the separation of DNAzyme-peptide from Fe_3O_4 through a simple magnetic separation. Based on a covalent bond interaction between peptide and the cysteine, the cleaved DNAzyme-peptide was captured onto the electrode surface and produced an electrochemical signal. Then, the enhanced electrocatalysis of DNAzyme toward H_2O_2resulted in the dramatic signal amplification. Also, the good conductivity and large surface are of $MoSe_2$@rGO contributed to the signal enhancement. As a consequence, highly sensitive detection of PSA was achieved by measuring the increase of current signal. More importantly, more than 3-fold enhancement in signal amplification was achieved due to peptide conjugation. This was the first application of hemin/G4 as electrocatalyst in "signal-on" electrochemical peptide biosensor. Owing to no requirement of extra redox mediator and protein enzyme, the biosensor potentially provided a cost-effective, simple yet highly sensitive assay for quantification of other proteins in clinical diagnosis.

2. Experimental section

2.1. Materials and reagents

Prostate specific antigen (PSA), hexanethiol (HT), gold chloride ($HAuCl_4$), sulfosuccinimidyl-4-(N-maleimidomethyl) cyclohexane-1-carboxylate (sulfo-SMCC), ammonium molybdate ($(NH_4)_2MoO_4$, 99.9%), poly (methacrylic acid sodium salt) (PMAA) and hemin were purchased from Sigma-Aldrich Chemical Co. (St. Louis, MO, USA). Graphene oxide (GO) was purchased from Nanjing Xian Feng Nano Co. (Nanjing, China). L-cysteine (Cys), selenium powder (Se, 99.5%), Oleic acid (OA) obtained from 1-ethyl-3-(3-dimethylaminopropyl) carbodiimide hydrochloride (EDC), N-Hydroxy succinimide (NHS) was purchased from J&K Scientific Ltd. (Beijing, China). $FeCl_3{\cdot}6H_2O$,

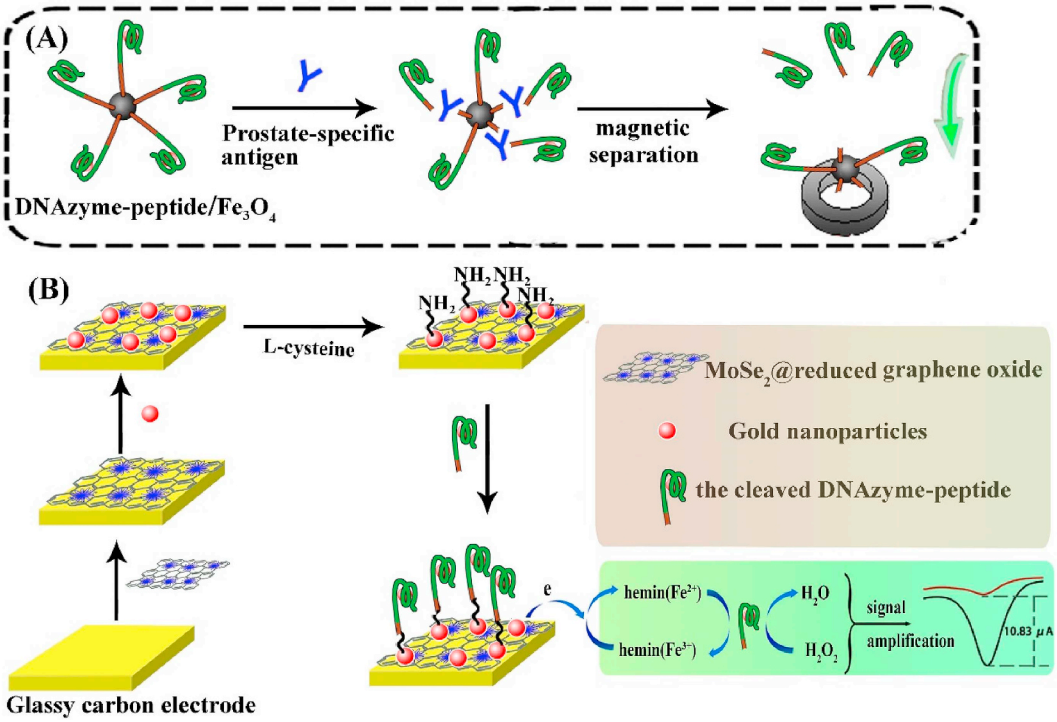

Scheme 1. (A) Schematic illustration for the preparation of DNAzyme-peptide/Fe_3O_4 probe and "signal-on" electrochemical peptide biosensor based on the versatile magnetic probe.

CH_3COONa (NaAc), ethylene glycol (EG) and 1,2-ethylenediamine (ETH), were purchased from Aladdin Co. Ltd. (Shanghai, China). A bifunctional peptide (CAAAHHHHHHEHSSKLQK) and control peptide (CAAAAAAAAAEHSSKLQK) were synthesized by Shanghai Science Peptide Biological Technology Co.; Ltd (Shanghai, China) and were received in lyophilized conditions. G-quadruplex (G4) (5′-GTGGGTAG GGCGGGTTGGA$_6$-NH_2-3′) was synthesized and purified by Sangon, Biotech Co.; Ltd. (Shanghai, China).

The buffer solutions used in this work were as follows. Phosphate buffered solution (PBS, pH 7.4, 0.1 M) was prepared with 0.1 M Na_2HPO_4 and 0.1 M KH_2PO_4, and 0.1 M KCl. Unless specified otherwise, PBS (pH 7.4) was used throughout the study. Tris-HCl buffer (20 mM, pH 7.4) containing 140 mM NaCl, 5 mM KCl, 1 mM $CaCl_2$ and 1 mM $MgCl_2$ was used as binding buffer. All buffer solutions were prepared using Milli-Q (18.2 MΩ · cm) water (Millipore) as a solvent. Except where noted, Milli-Q water was used in all the experiments. All the reagents were of analytical grade and directly used as received. Human serum used for real sample analysis was obtained from the First Affiliated Hospital of Zhengzhou University (Henan, China).

2.2. Apparatus and experimental measurements

Differential pulse voltammetry (DPV), cyclic voltammetry (CV) and electrochemical impedance spectroscopy (EIS) measurements, were performed on a CHI 650A electrochemical workstation (Shanghai Chenhua Instrument, China). A three-electrode system contained a modified glassy carbon working electrode (Φ = 4 mm), a platinum counter electrode and an Ag/AgCl reference electrode. The pH measurements were carried out with a PHS-3C precision pH meter (Shanghai, China). The scanning electron micrographs were taken with transmission electron microscope (TEM, USA FEI, M3000) and scanning electron microscope (SEM, JEOL, JSM-7500F). Infrared spectra datas were collected on a NEXUS-470 Fourier transform infrared (FT-IR) spectrometer (Thermo Electron, America).

All electrochemical experiments were conducted in a conventional electrochemical cell with three-electrode arrangement. CV experiments were performed in 2 mL $[Fe(CN)_6]^{3-/4-}$ (5.0 mM) containing KCl (0.1 M) with the potential scans between −0.2 and 0.7 V at the scan rate of 50 mV s^{-1}. DPV experiments were performed in 2 mL PBS (0.1 M, pH 7.0) containing 2.5 mM H_2O_2 within the potential range from 0.1 to −0.6 V. The conjugation of bifunctional peptide with G-quadruplex DNA was verified by electrophoresis analysis on 12% nondenaturing polyacrylamide gel (PAGE). Electrophoresis was carried out in 1 × TBE (pH 8.3) at a 100 V constant voltage for 75 min. After staining with ethidium bromide for 30 min, the gel were photographed on a G:BOX Chemi XT4 imaging system (Syngene, UK).

2.3. Synthesis of $MoSe_2$@rGO and Fe_3O_4–COOH

The $MoSe_2$@rGO nanocomposites were prepared according to a previously reported method with a little modification as follows [31]: firstly, $(NH_4)_2MoO_4$ (98 mg) and Se powder (79 mg) were dissolved in a mixture of 9 mL oleic acid, 5 mL ethanol and 4 mL GO (5 mg/mL) aqueous solution under vigorous stirring. Next, the mixture was transferred into a 20 mL Teflon autoclave reactor and reacted for 72 h at 200 °C, and then cooled down to room temperature. After centrifugation and washing with ethanol, the obtained products were dried in a vacuum at 60 °C overnight. To remove the organic residue and excess selenium powder, the as-prepared products were annealed in Ar/H_2 (95%:5%) at 300 °C for 2 h. Prior to use, 1 mg of prepared $MoSe_2$@rGO nanocomposites were suspended in 1 mL of absolute ethanol and sonicated to obtain a homogeneous suspension for the following experiment.

A simple solvothermal method reported by Guo et al. [32] was used for the preparation of carboxylate-functionalized Fe_3O_4 spheres (Fe_3O_4–COOH). Briefly, $FeCl_3{\cdot}6H_2O$ (1g) was first dissolved in EG (20 mL) to obtain a solution. Afterward, NaAc (3 g) and ETH (10 mL) were added the above solution and stirred for 30 min. The resulting mixture was sealed in a Teflon autoclave reactor, which was heated for 8 h at 200 °C in an oven. The product (i.e. Fe_3O_4) was thoroughly washed with water and was separated by magnet. Subsequently, 30 mg of Fe_3O_4 were re-dispersed in 50 mL water and 3 mL of PMAA (30%) were added into the solution, followed by sonication for 1 h. After keeping unperturbed overnight, Fe_3O_4–COOH could be obtained by magnetic separation. The final products were dissolved in 3 mL water for the following experiments.

2.4. Preparation of DNAzyme-peptide and magnetic DNAzyme-peptide-Fe_3O_4 probe

Peptide-conjugated G4 DNAzyme (DNAzyme-peptide) was prepared as described in our previous study [20], except for addition of bifunctional peptide as a substitute for cationic peptide. Briefly, with the amino group-active and sulfhydryl group-active sulfo-SMCC as crosslinker, cysteine-terminated peptide could be coupled with amino-terminated G4 structure. Additionally, another control peptide consisting of PSA-binding peptide motif and neutral peptide motif, was used to prepare the control magnetic probe according to the above method, so as to validate the enhancement function of bifunctional peptide toward DNAzyme activity.

To label DNAzyme-peptide with magnetic sphere, Fe_3O_4–COOH spheres (500 μL, 5 mg/mL) were firstly activated by EDC (20 mg/mL) and NHS (10 mg/mL). After separation by an external magnet, the Fe_3O_4 spheres were washed with PBS and then mixed with DNAzyme-peptide (500 μL, 10 μM) under stirring for 6 h at room temperature. During the time, the activated –COOH of Fe_3O_4 reacted with the amino group of lysine (K) at the C-terminus via acylation reaction, resulting in the formation of magnetic DNAzyme-peptide-Fe_3O_4 probe. The magnetic probes were collected by another magnetic separation and rinsed with PBS to remove unbound DNAzyme-peptide. Lastly, DNAzyme-peptide-Fe_3O_4 probes were re-suspended in 1 mL of PBS and stored at 4 °C for further use.

2.5. Preparation of functionalized electrode

Bare GCE was first pretreated by polishing with 0.3 and 0.05 mm alumina powder to obtain a mirror-like surface, followed by washing with ultrapure water thoroughly. To remove the residual alumina particles, GCE was sonicated in ethanol and ultrapure water in turn. Then, 10 μL of $MoSe_2$@rGO (1 mg/mL) were dropped onto the cleaned GCE surface. The modified electrode ($MoSe_2$@rGO/GCE) was dried at room temperature and was then electrodeposited at −0.2 V for 15 s in $HAuCl_4$ solution (1 wt%) to obtain gold nanoparticles (AuNPs)-modified substrate. Following that, the electrode was soaked in solution of L-cysteine (Cys, 10 mM) for 10 h at room temperature. At this time, Cys was assembled on the surface of Au nanoparticle based on the strong affinity between –SH and Au. At last, the prepared modified electrode was block with HT (1.0 mM). After each step, the modified electrode was thoroughly cleaned with PBS. The functionalized electrode was capable of capturing –COOH–containing biomolecule due to the presence of $–NH_2$ group from Cys, and it was stored at 4 °C when not used.

2.6. Sensing procedure of peptide as probe for PSA

DNAzyme-peptide-Fe_3O_4 (30 μL) probes were incubated with PSA targets at different concentrations and the mixture was placed on a shaker for 50 min with gentle tilting and rotating at 37 °C. In the meantime, PSA cleaved the protein-recognition peptide motif. After magnetic separation, the cleaved DNAzyme-peptide probes were added to a solution containing EDC (20 mg/mL) and NHS (10 mg/mL). The mixture was shaken for 2 h at room temperature to activate the –COOH in the side chain of glutamic acid (E) residues. Then, the functionalized

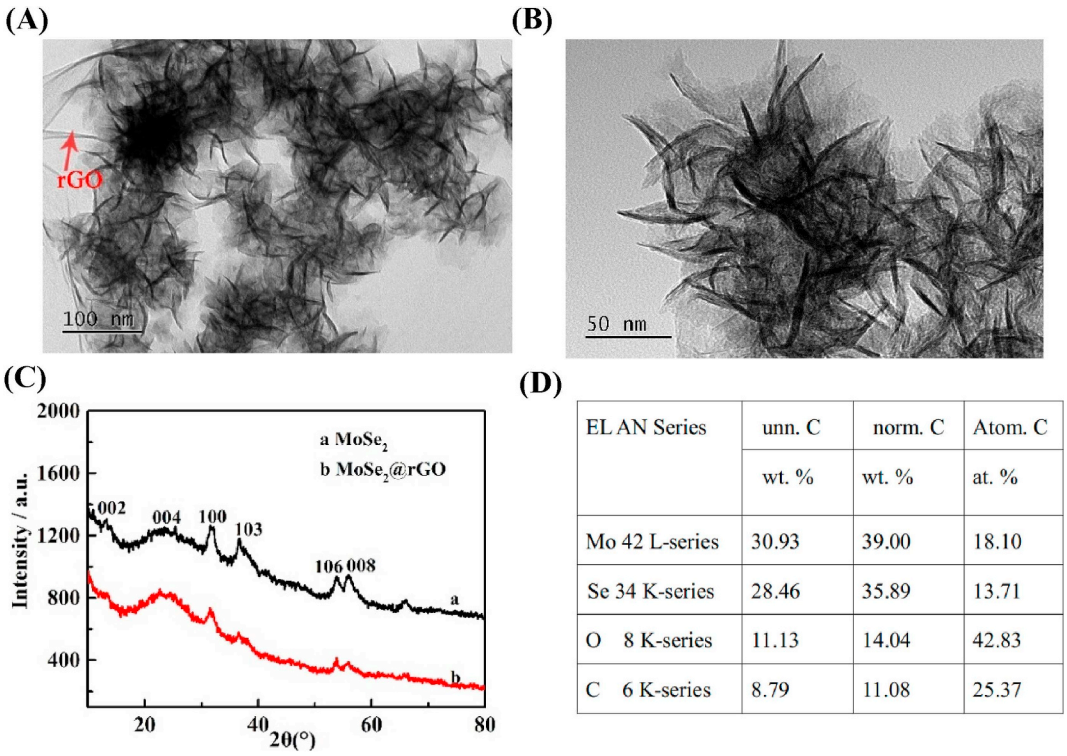

EL AN Series	unn. C	norm. C	Atom. C
	wt. %	wt. %	at. %
Mo 42 L-series	30.93	39.00	18.10
Se 34 K-series	28.46	35.89	13.71
O 8 K-series	11.13	14.04	42.83
C 6 K-series	8.79	11.08	25.37

Fig. 1. (A) TEM $MoSe_2$@rGO; (D) High-magnification TEM image of $MoSe_2$ grown on rGO; (C) X-ray diffraction pattern of (a) pure $MoSe_2$ and (b) $MoSe_2$@rGO hybrid; (D) EDS dates of $MoSe_2$@rGO.

electrode was incubated with the activated DNAzyme-peptide for 1 h to covalently immobilize DNAzyme-peptide through the interaction between –COOH of peptide and $–NH_2$ of Cys. After rinsed with PBS to remove the unbound DNAzyme-peptide, the modified electrode was used for DPV measurement. Finally, an electrochemical signal related to target PSA concentration was obtained due to the presence of redox-active hemin on the sensing interface. After adding H_2O_2 into the testing buffer solution, the signal was amplified obviously. By virtue of the relationship between the amplified signal and target concentration, quantitative analysis of PSA was achieved.

3. Results and discussion

3.1. Materials characterization

TEM characterization was first performed in order to evaluate the morphology of $MoSe_2$@rGO. The TEM images in Fig. 1A showed 3D $MoSe_2$ grew on rGO to form $MoSe_2$@rGO hybrid. The rosebud-like of nanostructure could be more clearly observed in Fig. 1B. In the XRD patterns of $MoSe_2$@rGO hybrid nanostructure, all the diffraction peaks of $MoSe_2$ (JCPDS: 29–0914) were also found (Fig. 1C), suggesting the reduced graphene oxide acted as the support substrate for growing $MoSe_2$. EDS analysis was further carried out to investigate the composition of $MoSe_2$@rGO hybrid (Fig. 1D), confirming that Mo, Se, C and O element existed in the composite. All the results indicated the $MoSe_2$@rGO hybrid was synthesized successfully.

The prepared Fe_3O_4 was characterized by TEM and it displayed a sphere morphology and mesoporous structure with an average size of about 70 nm (Fig. 2A). The inset in Fig. 2A showed that the Fe_3O_4 was well-dispersion and had the function of magnetic separation. To provide direct evidence for carboxyl functionalization on the Fe_3O_4, the FTIR Spectra was used to characterize the magnetic spheres. As shown in Fig. 2B, the strong IR band at 590 cm^{-1} was assigned to Fe–O vibrations [33]. The bands at 1408 cm^{-1} and 1629 cm^{-1} were corresponding to the carboxyl groups symmetric and antisymmetric stretching, respectively, and the bands at 3440 cm^{-1} was attributed to the hydroxyl group of carboxylic acid [34]. Especially, the pronounced carboxylic group could be observed at 1709 cm^{-1}. Combing TEM and FTIR, we concluded that PMAA with –COOH groups has been attached on the surface of mesoporous magnetic nanoparticles.

Native polyacrylamide gel electrophoresis (PAGE, 12%) was performed to prove the successful conjugation of peptide to G4 structure. As shown in Fig. 2C, the original G4 structure displayed an apparent band (Lane a). However, after modification of G4 structure with peptide, a band with a lower mobility from the notch (Lane b) can be observed, indicating the successful formation of DNAzyme-peptide hybrid. In addition, we preformed the circular dichroism (CD) measurement assay to characterize the structure of DNAzyme-peptide and explore the role of peptide. As shown in Fig. 2D, the original G4 presented a negative peak around 244 nm, a positive peak around 263 nm and a small positive peak at 298 nm, which indicated that both parallel and antiparallel structure co-existed in the G-quadruplexes (curve a) [35]. And then the CD intensity near 244 nm and 263 nm increased obviously after conjugation of peptide (curve b). In the meanwhile, the positive peak at 298 nm assigned to the characteristic of antiparallel G4 [36], almost disappeared in curve b. The observation revealed that antiparallel G4 transformed into the parallel counterparts and the DNAzyme-peptide almost existed in the form of parallel structure. Since parallel G4 structure was known to show better catalytic activity than the antiparallel G4, we concluded that the peptide conjugation really resulted in the activity enhancement of this DNAzyme due to its positive effect on the formation of parallel G4 [19].

3.2. Electrochemical characterization of functionalized electrode

To characterize the fabrication of peptide biosensor, the signals of $[Fe(CN)_6]^{3-/4-}$ probe at each modified electrode were recorded by cyclic voltammetry. As shown in Fig. 3, characteristic redox peaks of $[Fe(CN)_6]^{3-/4-}$ were first observed at the bare GCE (curve a). Compared with curve a, the peak current in curve b rose obviously, which

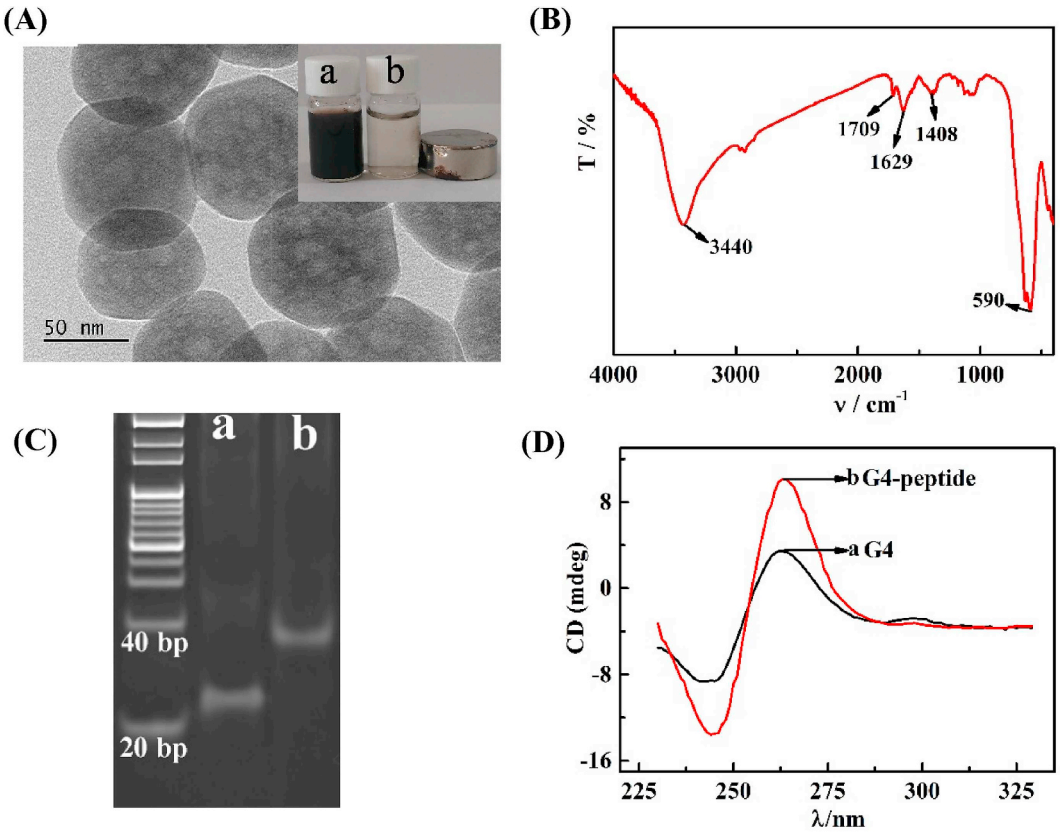

Fig. 2. (A) TEM images and (B) FT-IR spectra of Fe_3O_4–COOH; Inset: (a) photographs of magnetic spheres dispersed in water and (b) it also can be gathered to the sidewall of the vial by an external magnet field; (C) 12% PAGE images of G4 (Lane a, 100 μM) and bifunctional peptide-conjugated G4 (Lane b, 100 μM); (D) The corresponding circular dichroism spectra (concentration at 10 μM).

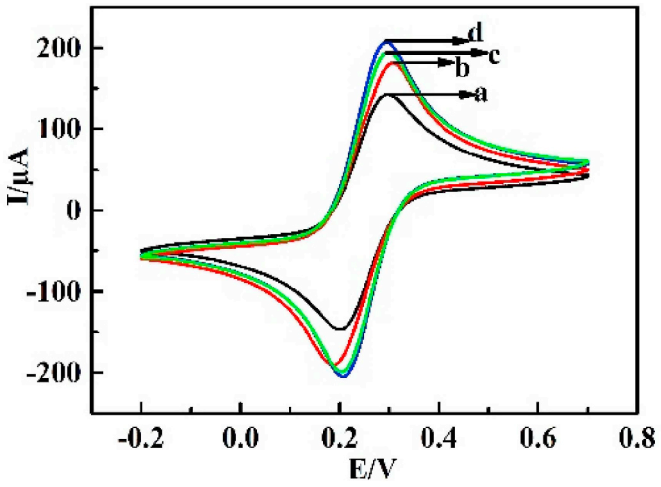

Fig. 3.

Fig. 3. Electrochemical characterization of peptide-based biosensor at different stages in PBS containing 5 mM $[Fe(CN)_6]^{3-/4-}$: (a) bare GCE; (b) $MoSe_2$@rGO/GCE; (c) depAu/$MoSe_2$@rGO/GCE; (d) Cys/depAu/$MoSe_2$@rGO/GCE.

indicated that the $MoSe_2$@rGO increased the effective surface area of electrode and exhibited the higher electrical conductivity. Sequent deposition of AuNPs resulted in the increase of current signal again (curve c), resulting from the good conductive property of AuNPs accelerating the electron transfer between the $[Fe(CN)_6]^{3-/4-}$ probe and electrode. In order to further confirm the assembly of AuNPs on the $MoSe_2$@rGO-modified electrode, the SEM images of $MoSe_2$@rGO and AuNPs/$MoSe_2$@rGO were performed (see Supporting Information Fig. S1). Compared with $MoSe_2$@rGO (Fig. S1(A)), the SEM image of AuNPs/$MoSe_2$@rGO (Fig. S1(B)) distinctly changed, on which AuNPs as spherical particles were attached to $MoSe_2$@rGO. When Cys was assembled onto the electrode, the current signal increased compared with that obtained at AuNPs/$MoSe_2$@rGO/GCE (Fig. 3, curve d vs curve c), suggesting that the positive charges from amino groups of Cys electrostatically contributed to the diffusion of negatively charged $[Fe(CN)_6]^{3-/4-}$ molecules to the electrode surface and Cys served as electron-transfer promoter [37]. The above results clearly proved that the functionalized electrode was fabricated as we expected.

3.3. Feasibility analysis

This work aimed at developing a simple yet highly sensitive peptide biosensor via a very effective signal amplification approach. So, we next investigated the electrochemical performance of this biosensor under different test conditions to evaluate the capability of the designed biosensor to amplify signal. In the absence of PSA, DNAzyme-peptide could not be separated from the magnetic Fe_3O_4 sphere. And then the upper suspension had no signal reporter (hemin) after magnetic separation. As expected, no detectable electrochemical signal was observed from the electrode (Fig. 4, curve a) in the applied potential range. However, the addition of target PSA resulted in the release of DNAzyme-peptide via PSA-induced peptide cleavage reaction. It was not unsurprising that the electrode provided an obvious response signal (Fig. 4, curve b) upon incubation of the DNAzyme-peptide-containing suspension. Notably, the electrochemical signal enhanced dramatically in the presence of H_2O_2 (Fig. 4, curve c), which indicated the excellent signal amplification performance of this biosensor. This gave witness to better sensitivity in this bioassay.

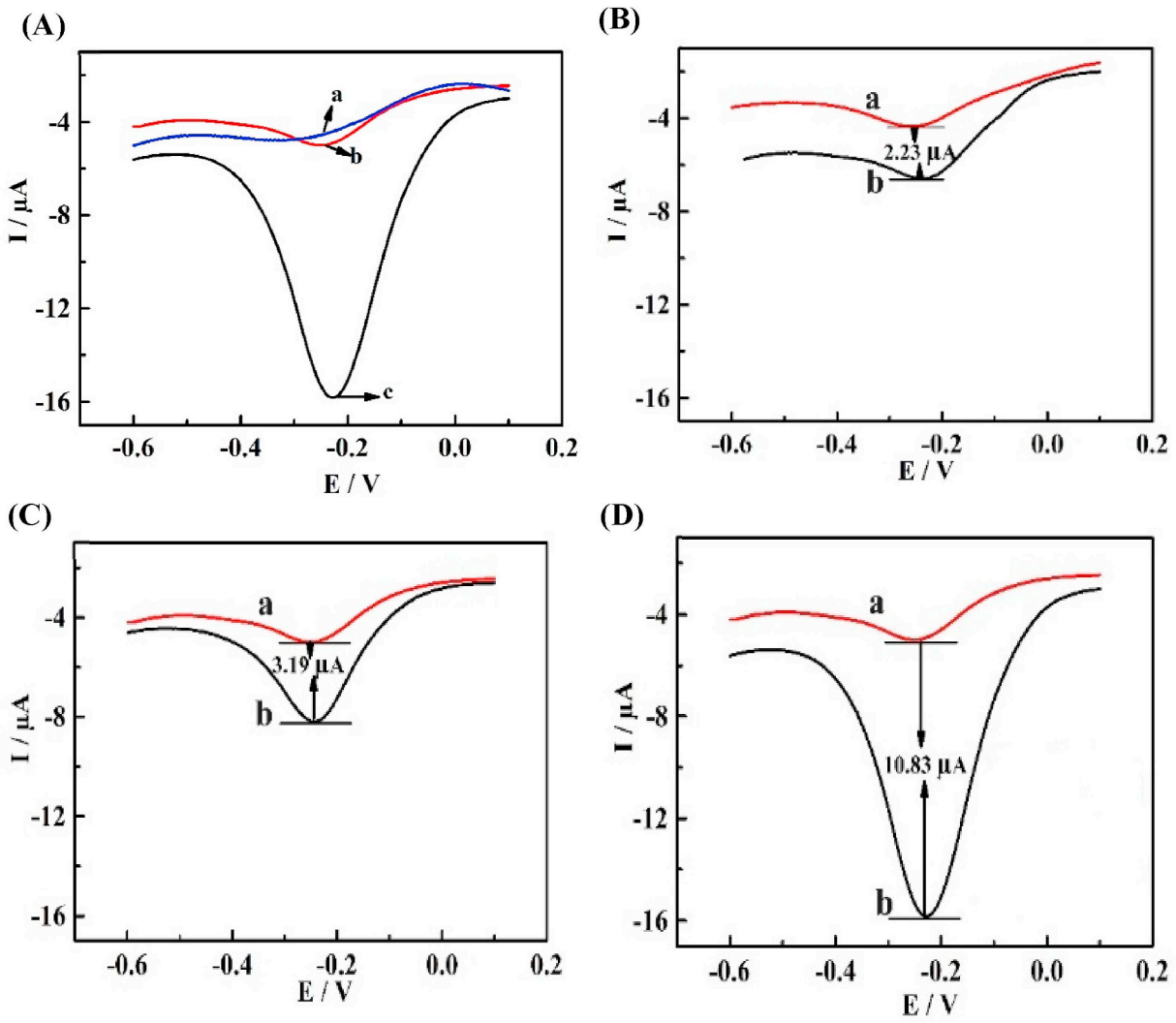

Fig. 4.

Fig. 4. (A) DPV response of the biosensor (a) without and (b) with target PSA in PBS (pH 7.4), (c) with target PSA in PBS containing H_2O_2; (B, C, D) DPV signals of different peptide biosensors before (curve a) and after (curve b) addition of H_2O_2: (B)without $MoSe_2$@rGO; (C) with the control magnetic probe; (D) the proposed magnetic probe.

3.4. Signal amplification of $MoSe_2$@rGO and DNAzyme-peptide

To ensure the aforementioned signal enhancement was attributed to the combined effect of DNAzyme-peptide and $MoSe_2$@rGO but not only one of them, we performed the control experiments to investigate the capability of each component in signal amplification. As shown in Fig. 4B and 2.23 μA of current difference (△I) before and after addition of H_2O_2 substrate, was observed at the functionalized electrode without $MoSe_2$@rGO, while it soared to 10.83 μA at $MoSe_2$@rGO-modified electrode (Fig. 4D). Such a comparison result suggested the good conductivity and larger surface area of $MoSe_2$@rGO, which could increase the electron transfer rate and provide more binding sites for immobilization of more DNAzyme-peptide. In the following control experiments, we expected to observe the enhanced electrocatalysis of DNAzyme-peptide in comparison with the original DNAzyme. As expected, the △I value at the electrode with the control magnetic probe was 3.19 μL, which was more that 3-fold lower than the value of 10.83 μL obtained at the proposed electrode (Fig. 4C vs. D). It clearly indicated that the proposed DNAzyme-peptide probe was able to efficiently enhance sensitivity. This also gave the key evidence that the peptide modification caused the improvement of peroxidase activity and led to a dramatic signal amplification. The activity enhancement might be ascribed to that cationic peptide modification not only stabilized anionic G4 structure and induced the formation of parallel G4 structure, just as the CD results indicated, but also improved the hemin binding affinity to G4 [38,39].

3.5. Quantification of PSA

After optimizing the assay conditions (see Supporting Information Fig. S2), we next studied the ability of the biosensor to sensitively detect PSA. In this strategy, the peptide conjugated to G4 structure was designed to be bifunctional, i.e., acting as DNAzyme activity enhancer and target PSA-recognition element. After adding PSA into Eppendorf tube, the magnetic probe was cleaved based on the specific recognition between PSA and PSA-binding peptide. After magnetic separation, the cleaved DNAzyme-peptide was covalently immobilized onto the electrode to offer a detectable signal. Interestingly, the signal was further amplified greatly owing to the enhanced electrocatalysis of DNAzyme-peptide. Therefore, the highly sensitive quantification of PSA was achieved based on a “signal-on” detection mode in this strategy. As shown in Fig. 5A, the current signal increased with the PSA increasing concentration (from a to k: 1.0×10^{-6}, 1.0×10^{-5}, 5.0×10^{-5}, 5.0×10^{-4}, 0.005, 0.05, 0.5, 5, 20, 80 ng/mL). And it was seen from

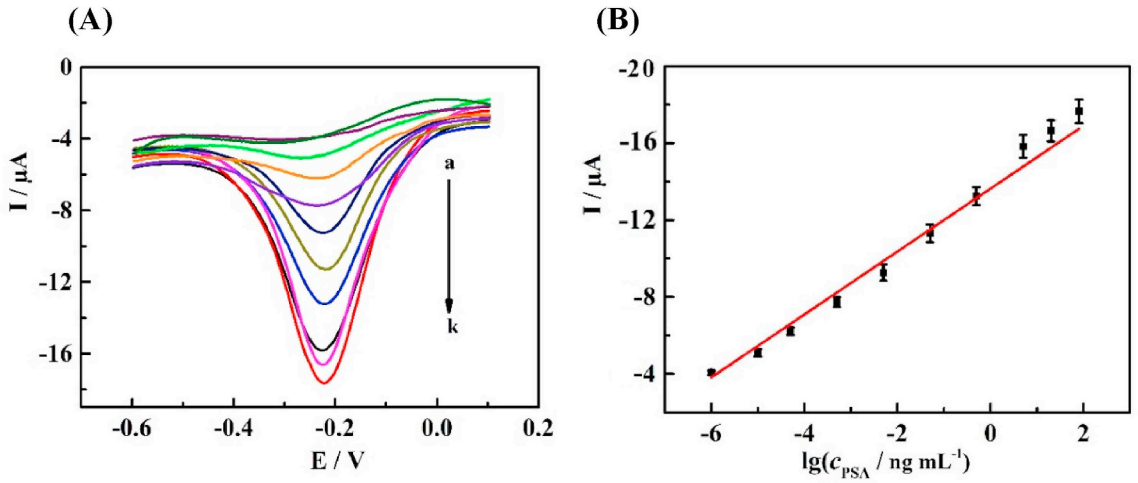

Fig. 5. (A) Quantification of PSA using signal-on peptide biosensor in 0.1 M PBS (pH 7.4) containing 2.5 mM H_2O_2(PSA concentration from a to k: 1.0×10^{-6}, 1.0×10^{-5}, 5.0×10^{-5}, 5.0×10^{-4}, 0.005, 0.05, 0.5, 5, 20, 80 ng/mL); (B) The calibration plots of current intensity versus the logarithm of target PSA concentrations. (Error bars, SD; n = 3).

Fig. 5B that the current intensity varied linearly with the logarithm of PSA concentration in the range of 1 fg/mL– 80 ng/mL, The linear equation was I = −1.636 lg C – 13.63 with a correlation coefficient of 0.9930 (C was the concentration of PSA). The detection limit was estimated to be 0.3 fg/mL (S/N = 3). As compared to other methods for the detection of PSA (Table S1) [7,11,40–43], the proposed strategy provided a wider linear range across seven orders of magnitude and lower detection limit, which was ascribed to the excellent electrocatalytic capability of DNAzyme-peptide and $MoSe_2$@rGO. Additionally, the biosensor was simpler and more low-cost, because no any protein enzyme, noble metal electrocatalyst and extra redox mediator were involved in the fabrication process. Moreover, the used peptide also served as G4 DNAzyme activity enhancer to improve the efficiency of signal amplification.

3.6. Selectivity, reproducibility and stability of the peptide biosensor

Several potential interferences including carcinoembryonic antigen (CEA), alpha-fetoprotein antigen (AFP), thrombin (TB) were employed as non-targets to prove the selectivity. As shown in Fig. 6, the current signal obtained from the electrode incubated with CEA (50 ng/mL), AFP (50 ng/mL) and TB (50 ng/mL) had no obvious difference with that from the blank group, while in the presence of PSA (either PSA or PSA-containing mixture), a distinct current signal was observed. This suggested that the proposed peptide biosensor detected PSA with good specificity even though in co-existence of interfering protein.

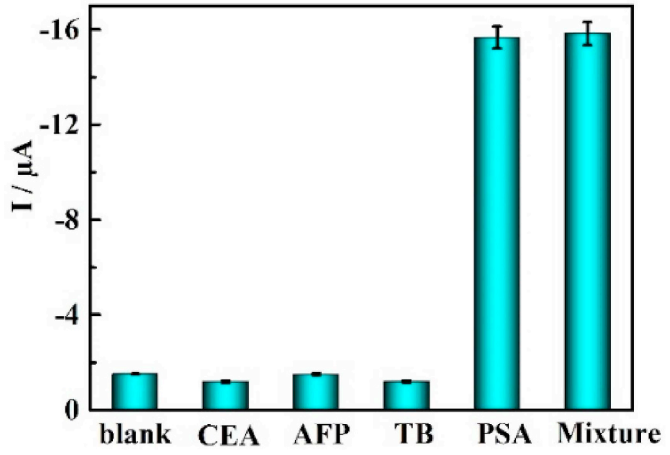

Fig. 6.

Fig. 6. Specificity of the peptide-based biosensor for PSA (5 ng mL^{-1}). The concentration of each interference was 50 ng mL^{-1}.

To evaluate the reproducibility of the biosensor, five independently electrodes were employed to detect the same concentration of PSA (5 ng/mL) under the same conditions. Similar current signal could be seen at the five electrodes and 6.60% of relative standard deviation (RSD) was obtained. And five repetitive measurements of PSA (5 ng/mL) yielded RSD of 6.10%. The intra-and inter-batch variation coefficients were all below 10%, indicating acceptable reproducibility of the biosensor. The stability was examined by measuring the response signal obtained at the as-prepared fresh electrode every five days (Fig. S3). After fifteen-day storage, the biosensor could still retain 92.29% of the initial current intensity, demonstrating good stability of the peptide biosensor.

3.7. Analysis of clinical serum samples

The practical application performance of the sensing platform was evaluated by detecting the levels of PSA in clinical serum samples. The serum sample was directly added to the Eppendorf tube containing magnetic probes and then was analyzed by the proposed biosensor. The obtained results were compared with those obtained by the electrochemiluminescence immunoassay as standard method (Table 1). The relative deviations ranged from −6.28% to 5.61%. The detected levels of PSA in several serum samples using this biosensor were in good agreement with the results obtained from standard method, indicating this biosensor provided an effective tool for detection of PSA in real biological samples.

Table 1
Comparison of serum PSA levels determined by using two methods.

serum samples	1	2	3	4	5
Electrochemical peptide biosensor [ng·mL^{-1}][a]	2.26	4.30	10.22	18.66	23.45
Electrochemiluminescence [ng/mL]	2.14	4.57	9.87	19.91	22.81
Relative deviation [%]	5.61	−5.91	3.55	−6.28	2.81

[a] Average value from three successive measurements.

4. Conclusions

This work described a novel peptide-based electrochemical method for PSA detection based on peptide-conjugated hemin/G4 and $MoSe_2$@rGO nanocomposites. It was the first report for G4 DNAzyme employed to develop an ultrasensitive "signal-on" electrochemical peptide biosensor. In this strategy, target protein detection, signal output and amplification were set in one-probe (i.e. DNAzyme-peptide-labeled magnetic probe), which rendered the method more sensitive, simple, low-cost. $MoSe_2$@rGO also conduced to the signal enhancement because of its good conductivity and large surface area. Consequently, the proposed biosensor presented much better detection performance for PSA and availably detected PSA in clinical serum samples. With the advantages of low reagent cost and simple operation, this strategy would provide a new approach for bioanalysis, facilitating the development of tool for early diagnosis of cancer in clinic.

Declaration of competing interest

No conflict of interest exits in the submission of this manuscript, and it is approved by all authors for publication. We certify that neither the entire paper nor any part of its content has been published or has been accepted elsewhere. It is not being submitted to any journal.

Acknowledgments

The authors are sincerely grateful for the financial support from the National Natural Science Foundation of China (No: 21575130).

Appendix A. Supplementary data

Supplementary data to this article can be found online at https://doi.org/10.1016/j.talanta.2019.120611.

References

[1] W.J. Castellani, Cancer (Prostate-Specific antigen), Anal. Chem. 67 (1995) 399–403.
[2] H.F. Gao, Q. Dang, S.Q. Xia, Y. Zhao, H.L. Qi, Q. Gao, C.X. Zhang, Highly selective electrogenerated chemiluminescence biosensor for simultaneous detection of matrix metalloproteinase-2 and matrix metalloproteinase-7 in cell secretions, Sens. Actuators B Chem. 253 (2017) 69–76.
[3] J.M. Lim, M.Y. Ryu, J.W. Yun, T.J. Park, J.P. Park, Electrochemical peptide sensor for diagnosing adenoma-carcinoma transition in colon cancer, Biosens. Bioelectron. 98 (2017) 330–337.
[4] J.Q. Liu, H. Cheng, D.G. He, X.X. He, K.M. Wang, Q.Q. Liu, S.Q. Zhao, X.D. Yang, Label-free homogeneous electrochemical sensing platform for protein kinase assay based on carboxypeptidase Y-assisted peptide cleavage and vertically ordered mesoporous silica films, Anal. Chem. 89 (2017) 9062–9068.
[5] H. Dai, S.H. Chen, Y.L. Li, B.S. Zeng, S.P. Zhang, Z.S. Hong, Y.Y. Lin, Photoelectrochemical biosensor constructed using TiO_2 mesocrystals based multipurpose matrix for trypsin detection, Biosens. Bioelectron. 92 (2017) 687–694.
[6] L.F. Yang, N. Li, K. Wang, X.M. Hai, J.X. Liu, F.Q. Dang, A novel peptide/Fe_3O_4@SiO_2-Au nanocomposite-based fluorescence biosensor for the highly selective and sensitive detection of prostate-specific antigen, Talanta 179 (2018) 531–537.
[7] Y. He, S.B. Xie, X. Yang, R. Yuan, Y.Q. Chai, Electrochemical peptide biosensor based on in situ silver deposition for detection of prostate specific antigen, ACS Appl. Mater. Interfaces 7 (2015) 13360–13366.
[8] H. Li, H.N. Xie, Y. Cao, X.R. Ding, Y.M. Yin, G.X. Li, A general way to assay protein by coupling peptide with signal reporter via supermolecule formation, Anal. Chem. 85 (2013) 1047–1052.
[9] B. Khalilzadeh, H.N. Charoudeh, N. Shadjou, R. Mohammad-Rezaei, Y. Omidi, K. Velaei, Z. Aliyari, M.R. Rashidi, Ultrasensitive caspase-3 activity detection using an electrochemical biosensor engineered by gold nanoparticle functionalized MCM-41: its application during stem cell differentiation, Sens. Actuators B Chem. 31 (2016) 561–575.
[10] P. Jing, H.Y. Yi, S.Y. Xue, R. Yuan, W.J. Xu, A 'signal on-off' electrochemical peptide biosensor for matrix metalloproteinase 2 based on target induced cleavage of a peptide, RSC Adv. 5 (2015) 65725–65730.
[11] S.B. Xie, J. Zhang, Y.L. Yuan, Y.Q. Chai, R. Yuan, An electrochemical peptide cleavage-based biosensor for prostate specific antigen detection via host–guest interaction between ferrocene and b-cyclodextrin, Chem. Commun. 51 (2015) 3387–3390.
[12] D. Wang, Y.L. Yuan, Y.N. Zheng, Y.Q. Chai, R. Yuan, An electrochemical peptide cleavage-based biosensor for matrix metalloproteinase-2 detection with exonuclease III-assisted cycling signal amplification, Chem. Commun. 52 (2016) 5943–5945.
[13] D. Wang, Y.Q. Chai, Y.L. Yuan, R. Yuan, A peptide cleavage-based ultrasensitive electrochemical biosensor with an ingenious two-stage DNA template for highly efficient DNA exponential amplification, Anal. Chem. 89 (2017) 8951–8956.
[14] X.Y. Li, J.J. Li, C.X. Zhu, X.H. Zhang, J.H. Chen, A new electrochemical immunoassay for prion protein based on hybridization chain reaction with hemin/G-quadruplex DNAzyme, Talanta 182 (2018) 292–298.
[15] Y.Q. Liu, E.H. Xiong, X.Y. Li, J.J. Li, X.H. Zhang, J.H. Chen, Sensitive electrochemical assay of alkaline phosphatase activity based on TdT-mediated hemin/G-quadruplex DNAzyme nanowires for signal amplification, Biosens. Bioelectron. 87 (2017) 970–975.
[16] G.F. Gan, B.F. Wang, J.Y. Huang, A. Qileng, Z.Y. He, H.T. Lei, W.P. Liu, Y.J. Liu, Multiple amplified enzyme-free electrochemical immunosensor based on G-quadruplex/hemin functionalized mesoporous silica with redox-active intercalators for microcystin-LR detection, Biosens. Bioelectron. 98 (2017) 126–133.
[17] Z.H. Wang, C.Y. Lu, J. Liu, J.J. Xu, H.Y. Chen, An improved G-quadruplex DNAzyme for dual-functional electrochemical biosensing of adenosines and hydrogen peroxide from cancer cells, Chem. Commun. 50 (2014) 1178–1180.
[18] S. Chen, P. Liu, K.W. Su, X. Li, Z. Qin, W. Xu, J. Chen, C.R. Li, J.F. Qiu, Electrochemical aptasensor for thrombin using co-catalysis of hemin/Gquadruplex DNAzyme and octahedral Cu_2O-Au nanocomposites for signal amplification, Biosens. Bioelectron. 99 (2018) 338–345.
[19] L. Xiao, Z.J. Zhou, M.L. Feng, A.J. Tong, Y. Xiang, Cationic peptide conjugation enhances the activity of peroxidase mimicking DNAzymes, Bioconjug. Chem. 27 (2016) 621–627.
[20] Y.M. Wu, G.P. Li, L.N. Zou, S. Lei, Q. Yu, B.X. Ye, Highly active DNAzyme-peptide hybrid structure coupled porous palladium for high-performance electrochemical aptasensing platform, Sens. Actuators B Chem. 259 (2018) 372–379.
[21] Y.M. Wu, L.N. Zou, S. Lei, Q. Yu, B.X. Ye, Highly sensitive electrochemical thrombin aptasensor based on peptide enhanced electrocatalysis of hemin/G-quadruplex and nanocomposite as nanocarrier, Biosens. Bioelectron. 97 (2017) 317–324.
[22] H. Li, H.N. Xie, N.N. Yang, Y. Huang, L.Z. Sun, G.X. Li, Design of a bi-functional peptide for protein assays: observation of cortactin expression in human placenta, Chem. Commun. 49 (2013) 5387–5389.
[23] Z.Q. Gao, Y.Y. Li, X.B. Zhang, J.H. Feng, L. Kong, P. Wang, Z.W. Chen, Y.H. Dong, Q. Wei, Ultrasensitive electrochemical immunosensor for quantitative detection of HBeAg using Au@Pd/MoS_2@MWCNTs nanocomposite as enzyme-mimetic labels, Biosens. Bioelectron. 102 (2018) 189–195.
[24] D. Zhu, W. Liu, D.X. Zhao, Q. Hao, J. Li, J.X. Huang, J.Y. Shi, J. Chao, S. Su, L.H. Wang, Label-free electrochemical sensing platform for microRNA-21 detection using thionine and gold nanoparticles Co-functionalized MoS_2 nanosheet, ACS Appl. Mater. Interfaces 9 (2017) 35597–35603.
[25] H.L. Shuai, K.J. Huang, Y.X. Chen, L.X. Fang, M.P. Jia, Au nanoparticles/hollow molybdenum disulfide microcubes based biosensor for microRNA-21 detection coupled with duplex-specific nuclease and enzyme signal amplification, Biosens. Bioelectron. 89 (2017) 989–997.
[26] T. Lin, L.S. Zhong, L.Q. Guo, F.F. Fu, G.N. Chen, Seeing diabetes: visual detection of glucose based on the intrinsic peroxidase-like activity of MoS_2 nanosheets, Nanoscale 6 (2014) 11856–11862.
[27] S. Su, H.F. Sun, W.F. Cao, J. Chao, H.Z. Peng, X.L. Zuo, L.H. Yuwen, C.H. Fan, L.H. Wang, Dual-target electrochemical biosensing based on DNA structural switching on gold nanoparticle-decorated MoS_2 nanosheets, ACS Appl. Mater. Interfaces 8 (2016) 6826–6833.
[28] H.L. Shuai, X. Wu, K.J. Huang, Z.B. Zhai, Ultrasensitive electrochemical biosensing platform based on spherical silicon dioxide/molybdenum selenide nanohybrids and triggered hybridization chain reaction, Biosens. Bioelectron. 94 (2017) 616–625.
[29] Z.Q. Liu, N. Li, H.Y. Zhao, Y.P. Du, Colloidally synthesized $MoSe_2$/graphene hybrid nanostructures as efficient electrocatalysts for hydrogen evolution, J. Mater. Chem. 3 (2015) 19706–19710.
[30] S.R. Denmeade, W. Lou, J. Lövgren, J. Malm, H. Lilja, J.T. Isaacs, Specific and efficient peptide substrates for assaying the proteolytic activity of prostate-specific antigen, Cancer Res. 57 (1997) 4924–4930.
[31] S.L. Xin, Z.Q. Liu, L. Ma, Y. Sun, C.H. Xiao, F. Li, Y.P. Du, Visualization of the electrocatalytic activity of three-dimensional $MoSe_2$@reduced graphene oxide hybrid nanostructures for oxygen reduction reaction, Nano Research 9 (2016) 3795–3811.
[32] S.J. Guo, D. Li, L.X. Zhang, J. Li, E.K. Wang, Monodisperse mesoporous superparamagnetic single-crystal magnetite nanoparticles for drug delivery, Biomaterials 30 (2009) 1881–1889.
[33] X.W. Yang, W. Jiang, L. Liu, B.H. Chen, S.X. Wu, D.P. Sun, F.S. Li, One-step hydrothermal synthesis of highly water-soluble secondary structural Fe_3O_4 nanoparticles, J. Magn. Magn. Mater. 324 (2012) 2249–2257.
[34] N. Alizadeh, R. Hallaj, A. Salimi, A highly sensitive electrochemical immunosensor for hepatitis B virus surface antigen detection based on hemin/G-quadruplex horseradish peroxidase-mimicking DNAzyme-signal amplification, Biosens. Bioelectron. 94 (2017) 184–192.
[35] P. Balagurumoorthy, S.K. Brahmachari, D. Mohanty, M. Bansal, V. Sasisekharan, Hairpin and parallel quartet structures for telomeric sequences, Nucleic Acids Res. 20 (1992) 4061–4067.
[36] W.J. Zhang, T.M. Qu, Y.J. Lu, Y.Y. Huang, W.B. Wu, Z.S. Huang, J.L. Zhou, K.Y. Wong, L.Q. Gu, 9-Substituted berberine derivatives as G-quadruplex stabilizing ligands in telomeric DNA, Bioorg. Med. Chem. 15 (2007) 5493–5501.
[37] L.M. Zhu, L.Q. Luo, Z.X. Wang, DNA electrochemical biosensor based on thionine-graphene nanocomposite, Biosens. Bioelectron. 35 (2012) 507–511.
[38] T.J. Chang, H.M. Gong, P. Ding, X.J. Liu, W.G. Li, T. Bing, Z.H. Cao,

D.H. Shangguan, Activity enhancement of G-quadruplex/hemin DNAzyme by flanking d(CCC), Chem. Eur J. 22 (2016) 4015–4021.
[39] C. Qi, N. Zhang, J.L. Yan, X.J. Liu, T. Bing, H.C. Mei, D.H. Shangguan, Activity enhancement of G-quadruplex/hemin DNAzyme by spermine, RSC Adv. 4 (2014) 1441–1448.
[40] Y.X. Dong, J.T. Cao, Y.M. Liu, S.H. Ma, A novel immunosensing platform for highly sensitive prostate specific antigen detection based on dual-quenching of photocurrent from CdSe sensitized TiO_2 electrode by gold nanoparticles decorated polydopamine nanospheres, Biosens. Bioelectron. 91 (2017) 246–252.
[41] J.C. Zhao, Z.F. Ma, Ultrasensitive detection of prostate specific antigen by electrochemical aptasensor using enzyme-free recycling amplification via target-induced catalytic hairpin assembly, Biosens. Bioelectron. 102 (2018) 312–320.
[42] H.L. Qi, M. Li, M.M. Dong, S.P. Tuan, Q. Gao, C.X. Zhang, Electrogenerated chemiluminescence peptide-based biosensor for the determination of prostate-specific antigen based on target induced cleavage of peptide, Anal. Chem. 86 (2014) 1372–1379.
[43] D.D. Xu, Y.L. Deng, C.Y. Li, Y. Lin, H.W. Tang, Metal-enhanced fluorescent dye-doped silica nanoparticles and magnetic separation: a sensitive platform for one-step fluorescence detection of prostate specific antigen, Biosens. Bioelectron. 87 (2017) 881–887.